



HAL
open science

Non-triangular self-synchronizing stream ciphers

Julien Francq, Loic Besson, Paul Huynh, Philippe Guillot, Gilles Millérioux,
Marine Minier

► **To cite this version:**

Julien Francq, Loic Besson, Paul Huynh, Philippe Guillot, Gilles Millérioux, et al.. Non-triangular self-synchronizing stream ciphers. *IEEE Transactions on Computers*, 2022, 71 (1), pp.134-145. 10.1109/TC.2020.3043714 . hal-03081725

HAL Id: hal-03081725

<https://hal.science/hal-03081725>

Submitted on 20 Jul 2021

HAL is a multi-disciplinary open access archive for the deposit and dissemination of scientific research documents, whether they are published or not. The documents may come from teaching and research institutions in France or abroad, or from public or private research centers.

L'archive ouverte pluridisciplinaire **HAL**, est destinée au dépôt et à la diffusion de documents scientifiques de niveau recherche, publiés ou non, émanant des établissements d'enseignement et de recherche français ou étrangers, des laboratoires publics ou privés.

Non-Triangular Self-Synchronizing Stream Ciphers

Julien Francq, Loïc Besson, Paul Huynh, Philippe Guillot, Gilles Millerioux and Marine Minier

Abstract—In this paper, we propose an instantiation, called *Stanislas*, of a dedicated Self-Synchronizing Stream Cipher (SSSC) involving an automaton with finite input memory using non-triangular state transition functions. Previous existing SSSC are based on automata with shifts or triangular functions (T -functions) as state transition functions. Our algorithm *Stanislas* admits a matrix representation deduced from a general and systematic methodology called Linear Parameter Varying (LPV). This particular representation comes from the automatic theory and from a special property of dynamical systems called flatness.

Hardware implementations and comparisons with some state-of-the-art stream ciphers on Xilinx FPGAs are presented. It turns out that *Stanislas* provides bigger throughput than the considered stream ciphers (synchronous and self-synchronizing) when straightforward implementations are considered. Moreover, its synchronization delay is much smaller than the SSSC *Moustique* (40 clock cycles instead of 105) and the standard approach CFB1-AES128 (40 clock cycles instead of 128).

Index Terms—Self-Synchronizing Stream Ciphers, automata with finite input memory, flatness, hardware implementations.

I. INTRODUCTION

Self-Synchronizing Stream Ciphers (SSSCs) were patented in 1946. The basic principle of such ciphers is to encrypt every plaintext symbol with a transformation that only involves a fixed number of previous ciphertext symbols. Therefore, every ciphertext symbol is correctly deciphered provided that previous symbols have been properly received. This self-synchronization property has many advantages and is especially relevant to group communications. In this respect, since 1960, specific SSSCs have been designed and are still used to provide bulk encryption (for Hertzian line, RNIS link, etc.) in military applications or governmental radio mobile networks [1], [2].

The canonical form of the SSSC combines a shift register, which acts as a state register with the ciphertext as input, together with a filtering function that provides the running key stream. The cryptographic complexity of the canonical

form of the SSSC lies in the filtering function. In the early 90s, studies have been performed [1], [3] to propose secure designs of SSSCs. These works have been followed by effective constructions ([4], [5], [6]). What motivates the present proposal for a new SSSC is that, till now, all of these SSSC schemes have been broken ([7], [8], [9], [10], [11]). And up to our knowledge, since 10 years, no other proposals of SSSCs has been made. Clearly, SSSCs can be naturally built using a block cipher by applying the Cipher Feedback (CFB) mode. However, the computational cost of CFB is one full block cipher operation per digit. So for single-bit digits, it is n times less efficient than synchronous stream encryption modes such as Output Feedback (OFB) or Counter (CTR) Mode, with n the block length. For example, AES in single-bit CFB mode (as defined as “CFB1-AES128” in NIST SP 800-38a [12]) is 128 times less efficient than AES in CTR mode. As a consequence, it seems interesting to propose dedicated SSSCs and consider them as a category of primitives on their own.

The aim of the present paper is to propose a new framework, along with an instantiation called *Stanislas*, to design SSSCs. The design approach is based on both the special feature of Finite State Machines admitting a matrix representation, called LPV (Linear Parameter Varying) automata and on a property of dynamical systems named flatness coming from control theory. Flatness is interpreted in terms of the structure of the adjacency matrix of a graph associated to the automaton from which self-synchronization can be easily characterized. The matrix representation is thus a generalization of Rational Linear Finite State Machines [13], [14]. The use of flatness for the sake of cryptography has been first proposed in [15]. It has been shown that flatness characterizes the self-synchronization property. Moreover, the matrix representation allows to design automata which can be more general than T -functions as it was the case over the past years (see [16], [6] as examples). One of the benefits of this approach is that we could introduce nonlinearities with proved properties in the matrix representation, what a shift register does not always permit. Due to this peculiarity, the class of admissible automata to act as SSSCs is thereby enlarged.

In the present paper, a complete cipher, called *Stanislas* (for Secure Transmission Algorithm with Non triangular Iterative Structure Looking After Self-synchronization) and designed from the LPV framework, is described. The Key Schedule, the design rationale and the security analysis are provided. Next, hardware implementation results on Xilinx FPGA platforms of *Stanislas* are performed and compared with some state-of-the art competitors: some

This work was partially supported by the French National Agency of Research under the grants number ANR-13-INSE-0005-01 and by the french PIA project “Lorraine Université d’Excellence”, reference ANR-15-IDEX-04-LUE.

Julien Francq and Loïc Besson were with Airbus CyberSecurity, 1 Bd Jean Moulin, CS 40001, MetaPole, 78996 Élancourt Cedex

Paul Huynh and Marine Minier are with Université de Lorraine, CNRS, Inria, LORIA, F-54000 Nancy, France, email: firstname.name@loria.fr

Philippe Guillot is with Université Paris 8, LAGA, UMR 7539, France, email: philippe.guillot@univ-paris8.fr

Gilles Millerioux is with Université de Lorraine, CNRS, CRAN, UMR 7039, France, email: gilles.millerioux@univ-lorraine.fr

Synchronous Stream Ciphers coming from eSTREAM portfolio (TRIVIUM [17] and Grain [18]), one SSSC (Moustique) and the only known feedback mode (the NIST-standardized CFB1-AES128). Interestingly, Stanislas provides the highest throughput on Xilinx Spartan-6 XC6SLX75T FPGAs compared to its stream ciphers and SSSC competitors, implemented in a straightforward manner. Moreover, with the same comparison conditions, its synchronization delay is much smaller than the SSSC Moustique (40 clock cycles instead of 105) and the standard approach CFB1-AES128 (40 clock cycles instead of 128), which provides a decisive advantage for applications when low-latency synchronization is required (e.g., Telecom).

The paper is organized as follows. Section II recalls the theoretical results linking together flatness and SSSC. Section III presents the new SSSC Stanislas. The design rationale and the security analysis are detailed in Section IV. Finally, Section V provides hardware implementation results and comparisons. Section VI concludes this paper.

II. THEORETICAL FOUNDATIONS AND FLATNESS

After few generalities on stream ciphers, it is recalled in this section the main results of [15] concerning the design of SSSC based on the property of flatness.

A. Generalities on Stream Ciphers

For a stream cipher, it must be given an alphabet A , that is, a finite set of basic elements named symbols. The set A stands in this paragraph as a general notation without any specific alphabet. Typically, A could be composed of 1 or several bits elements. Hereafter, the index $t \in \mathbb{N}$ will stand for the discrete-time. On the transmitter part, the plaintext (also called information or message) $m \in \mathcal{M}$ (\mathcal{M} is the message space) is a string of plaintext symbols $m_t \in A$. Each plaintext symbol is encrypted, by means of an encryption (or ciphering) function e , according to:

$$c_{t+r} = e(z_{t+r}, m_t), \quad (1)$$

where $z_t \in A$ is a so-called keystream (or running key) symbol delivered by a keystream generator. The function e is invertible for any prescribed z_t . The resulting symbol $c_t \in A$ is the ciphertext symbol. The integer $r \geq 0$ stands for a potential delay between the plaintext m_t and the corresponding ciphertext c_{t+r} . This is explained by computational or implementation reasons, see [16] for example. Consequently, for stream ciphers, the way how to encrypt each plaintext symbol changes on each iteration. The resulting ciphertext $c \in \mathcal{C}$ (\mathcal{C} is called the ciphertext space), that is the string of symbols c_t , is conveyed to the receiver through a public channel.

At the receiver side, the ciphertext c_t is deciphered according to a decryption function d which depends on a running key $\hat{z}_t \in A$ delivered, similarly to the cipher part, by a keystream generator. The decryption function d obeys the following rule. For any two keystream symbols $\hat{z}_{t+r}, z_{t+r} \in A$, it holds that

$$\hat{m}_{t+r} := d(c_{t+r}, \hat{z}_{t+r}) = m_t \text{ whenever } \hat{z}_{t+r} = z_{t+r}. \quad (2)$$

Equation (2) means that the running keys z_t and \hat{z}_t must be synchronized for a proper decryption. The generators delivering the keystreams are parametrized by a secret key denoted by $K \in \mathcal{K}$ (\mathcal{K} is the secret key space). The distinct classes of stream ciphers (synchronous or self-synchronizing) differ each other by the way on how the keystreams are generated and synchronized. Next, we detail the special class of stream ciphers called Self-Synchronizing Stream Ciphers.

B. Keystream Generators for Self-Synchronizing Stream Ciphers

A well-admitted approach to generate the keystreams has been first suggested in [1]. It is based on the use of so-called finite state automata with finite input memory as described below. This is typically the case in the cipher Moustique [19]. At the ciphering side, the automaton delivering the keystream takes the form:

$$\begin{cases} x_{t+1} = f_K(x_t, m_t), \\ z_{t+r} = h_K(x_t) \end{cases} \quad (3)$$

where $x_t \in A$ is the internal state, f is the next-state transition function parametrized by $K \in \mathcal{K}$. As previously stressed, the delay b is introduced to cope with special situations, in particular when the computation of the output (also called filtering) delivered by the function h involves r successive operations processed at time instants $t, \dots, t+r$. Those operations will be here matrix multiplications as detailed later in Equation (14). Substituting m_t by its expression (2) yields an automaton described by

$$\begin{cases} x_{t+1} = g_K(x_t, c_{t+r}), \\ z_{t+r} = h_K(x_t) \end{cases} \quad (4)$$

If such an automaton has finite input memory, it means that, by iterating (4) a finite number of times, there exists a function ℓ_K and a finite integer M such that

$$x_t = \ell_K(c_{t+r-1}, \dots, c_{t+r-M}), \quad (5)$$

and thus,

$$z_{t+r} = h_K(\ell_K(c_{t+r-1}, \dots, c_{t+r-M})). \quad (6)$$

Actually, the fact that the keystream symbol can be written in the general form

$$z_{t+r} = \sigma_K(c_{t-\ell}, \dots, c_{t-\ell'}), \quad (7)$$

with σ_K a function involving a finite number of past ciphertexts from time $t-\ell$ to $t-\ell'$ ($\ell, \ell' \in \mathbb{Z}$), is a common feature of the SSSC. Equation (7) is called the canonical equation.

Remark 1: The benefits of implementing the recursive forms (3) or (4) instead of directly implementing the canonical form (7) is that we can obtain nonlinear functions σ_K of high complexity by implementing simpler nonlinear functions f_K or g_K . The complexity results from the successive iterations which act as composition operations.

At the deciphering side, the automaton takes the form

$$\begin{cases} \hat{x}_{t+1} = g_K(\hat{x}_t, c_{t+r}), \\ \hat{z}_{t+r} = h_K(\hat{x}_t) \end{cases} \quad (8)$$

where \hat{x}_t is the internal state. Similarly to the cipher part, the automaton having a finite input memory, it means that, by iterating Equation (8) a finite number of times, one also obtains

$$\hat{x}_t = \ell_K(c_{t+r-1}, \dots, c_{t+r-M}),$$

and thus,

$$\hat{z}_{t+r} = h_K(\ell_K(c_{t+r-1}, \dots, c_{t+r-M})).$$

Hence, it is clear that after a transient time of maximal length equal to M , it holds that, for $t \geq M$,

$$\hat{x}_t = x_t \text{ and } \hat{z}_{t+r} = z_{t+r}. \quad (9)$$

In other words, the generators synchronize automatically after at most M iterations. Hence, the decryption is automatically and properly achieved after at most M iterations too. No specific synchronizing protocol between the cipher and the decipher is needed. This explains the terminology Self-Synchronizing Stream Ciphers. The integer M is called the synchronization delay.

Hereafter, the considered automata will be assumed to operate on the q elements finite field $\mathbb{F} = \mathbb{F}_q$ where q is a prime power.

C. Flat LPV Automata and SSSC

For the automaton described by (3) (or the equivalent automaton described by (4) after substitution) to get a finite input memory feature (see (5)), the solutions proposed in the open literature call for state transition functions g_K in the form of shifts or more generally T -functions (T for Triangle). It is recalled that T -functions are functions that propagate dependencies in one direction only. Till now, none of the proposed SSSCs has involved non-triangular state transition functions although T -functions are known to suffer from weaknesses [9]. Indeed, T -functions induce a propagation of differential properties which make them easier to cryptanalyse. It is explained by the fact that no systematic methodology for constructing finite automata with finite input memory and involving general non-triangular state transition functions was proposed so far. Actually, in [15], a particular class of automata called flat LPV (Linear Parameter-Varying) has been introduced and it has been shown that this class allows to define such an expected systematic methodology. Let us recall what is a flat automaton.

Definition 1: An automaton described by the dynamics f verifying

$$x_{t+1} = f(x_t, m_t) \quad (10)$$

where $x_t \in \mathbb{F}^n$ is the state, $m_t \in \mathbb{F}$ is the input, is said to be flat, if there exists a function

$$\begin{aligned} h : \mathbb{F}^n \times \mathbb{F} &\rightarrow \mathbb{F} \\ c_t &= h(x_t, m_t) \end{aligned}$$

such that all system variables can be expressed as a function of c_t and a finite number of its backward and forward shifts.

The output c_t is called the flat output. Hence, by definition, there exists a function \mathcal{F} such that

$$x_t = \mathcal{F}(c_{t+t_0}, \dots, c_{t+t_1}) \quad (11)$$

where t_0 and t_1 are \mathbb{Z} -valued integers. A central remark is that (11) is nothing but the canonical equation of an SSSC (compare with (5)). As a direct consequence, a flat automaton is equivalent to being an SSSC and thus is central for design perspectives.

LPV automata, defined over a field \mathbb{F} , are described by the following state space representation:

$$x_{t+1} = A_{\rho(t)}x_t + Bm_t \quad (12)$$

$x_t \in \mathbb{F}^n$ is the state vector, $m_t \in \mathbb{F}$ is the input. The matrices $A \in \mathbb{F}^{n \times n}$ and $B \in \mathbb{F}^{n \times 1}$ are respectively the dynamical matrix and the input matrix. The output c_t is defined as

$$c_t = Cx_t \quad (13)$$

with $C \in \mathbb{F}^{1 \times n}$ the output matrix. The matrix B is the input matrix and defines the component x_t^i on which the symbol m_t is added. Let us note that m_t can be added to several components. Such a system is called Linear Parameter-Varying because it is written with a linear dependency with respect to the state vector. The set of all varying parameters of A are collected on a vector denoted by

$$\rho(t) = [\rho^1(t), \rho^2(t), \dots, \rho^L(t)] \in \mathbb{F}^L$$

where L is the total number of non-zero (possibly varying) entries. Such automata can exhibit nonlinear dynamics. Indeed, the nonlinearity is obtained by defining the varying parameters $\rho^i(t)$ as nonlinear functions $\varphi^i : \mathbb{F}^{s+1} \rightarrow \mathbb{F}$ of the output c_t (or a finite number of shifts) $\rho^i(t) = \varphi^i(c_t, c_{t-1}, \dots, c_{t-s})$ with s a natural number. Let us notice that the notation $\rho^i(t)$ (usual in the literature for LPV systems) is somehow abusive because it does not reflect an explicit dependency with respect to the time t but on quantities, here c_t , indexed with t . Furthermore, the LPV structure is suitable to construct non triangular state transition functions. Indeed, because of the varying entries, the state transition function is not triangular if there does not exist a common and constant triangularization basis over the whole set of matrices $A_{\rho(t)}$ with $\rho(t) \in \mathbb{F}^L$. Hence, it suffices to select the position of the varying parameters $\rho^i(t)$ in the matrix A accordingly.

As a simple illustration, the automaton governed by Equation (12) with the setting

$$A_{\rho(t)} = \begin{pmatrix} a & 0 & 1 \\ \rho^1(t) & \rho^2(t) & 0 \\ a & 1 & 1 \end{pmatrix}, \quad B = \begin{pmatrix} 1 \\ 0 \\ 0 \end{pmatrix}$$

with a a constant element in \mathbb{F} , $\rho^1(t) = c_t \cdot c_{t-1}$ and $\rho^2(t) = (c_{t-2})^2$, is an LPV automaton and does not admit a constant triangularization basis.

A flat LPV automaton is an LPV automaton of which state vector x_t verifies (11).

Let us recall from [15] the main proposition which allows to define a family of SSSCs based on LPV automata. For brevity, we introduce the following notation. For $t_2 \geq t_1$, denote by $\prod_{l=t_2}^{t_1} A_{\rho(l)}$ the product of matrices $A_{\rho(l)}$ from t_2 to t_1 . For $t_2 < t_1$, define $\prod_{l=t_2}^{t_1} A_{\rho(l)} = \mathbf{1}_n$ (the identity matrix of dimension n). Finally, let \mathcal{T} be the scalar defined by $\mathcal{T} = C \prod_{l=t+1}^{t+r-1} A_{\rho(l)} B$.

Proposition 1: If the LPV finite state automaton defined by (12) is flat, defining the keystream with delay r as

$$z_{t+r} = C \prod_{l=t+r-1}^t A_{\rho(l)} x_t \quad (14)$$

and the ciphering function as

$$c_{t+r} = z_{t+r} + \mathcal{T} m_t, \quad (15)$$

the set of equations (12), (14) and (15) define the ciphering part of an SSSC.

On the other hand, consider the finite state automaton with internal state \hat{x}_t with dynamics given by

$$\hat{x}_{t+1} = P_{\rho(t:t+r)} \hat{x}_t + B \mathcal{T}^{-1} c_{t+r} \quad (16)$$

with

$$P_{\rho(t:t+r)} = A_{\rho(t)} - B \mathcal{T}^{-1} C \prod_{l=t+r-1}^t A_{\rho(l)} \quad (17)$$

along with the keystream \hat{z}_t defined as

$$\hat{z}_{t+r} = C \prod_{l=t+r-1}^t A_{\rho(l)} \hat{x}_t \quad (18)$$

and the deciphering function obeying

$$\hat{m}_{t+r} = \mathcal{T}^{-1} (c_{t+r} - \hat{z}_{t+r}). \quad (19)$$

Then, the set of equations (16-19) define the deciphering part of an SSSC.

The proof given in [15] consists in showing that, if the LPV finite state automaton defined by (12) is flat, then there exists an integer M such that the synchronization error $x_k - \hat{x}_{t+r}$ reaches zero after a finite transient time of length M . The integer M is the synchronization delay. Actually, it is shown that flatness is equivalent to the existence of an integer M such that for all $t \geq 0$,

$$P_{\rho(t+M-1:t+M-1+r)} P_{\rho(t+M-2:t+M-2+r)} \cdots P_{\rho(t:t+r)} = 0 \quad (20)$$

where the product (20) results from the composition of the state transition functions of the deciphering automaton. Let us note that T and r are independent.

This LPV framework for the design of SSSC is new regarding the literature devoted to the design of SSSC. In particular, it really differs from the serial and parallel constructions proposed in the 90s by Maurer [1].

According to Remark 1, implementing the recursive form (12) and (16) instead of the canonical form (5) is more efficient from a computational point of view.

It is recalled that the non-linearity is obtained by defining the values of every varying parameters $\rho^i(t)$ ($i = 1, \dots, L$) involved in the matrices of (12-19) as non-linear functions φ^i of a finite number of past cryptograms

($\rho^i(t) = \varphi^i(c_t, c_{t-1}, \dots, c_{t-s})$). Those functions will be implemented in the form of S-boxes denoted S .

$$\begin{aligned} \varphi^i : \mathbb{F}^{s+1} &\rightarrow \mathbb{F} \\ (c_t, c_{t-1}, \dots, c_{t-s}) &\mapsto S(c_t, c_{t-1}, \dots, c_{t-s}, SK_i) \end{aligned} \quad (21)$$

where SK_i is the subkey number i derived from the secret key denoted with K .

The point is that the LPV automaton defined by (12) must be flat for any secret key K and any realization of $\rho(t)$. In other words, flatness must be a generic property of (12). Designing an LPV automaton (12) which is generically flat relies on an admissible realization of a corresponding structured linear system. A structured linear system is a linear system only defined by the sparsity pattern of the state space realization matrices. In other words, for a structured linear system, we distinguish between the entries that are fixed to zero and the other ones that can take any value in \mathbb{F} , including the ones which are time-varying. Hence, a structured linear discrete-time system, denoted by Σ_Λ , is a system that admits the form:

$$\Sigma_\Lambda : x_{t+1} = I_A x_t + I_B m_t. \quad (22)$$

The entries of the matrices of (22) are ‘0’ or ‘1’. In particular, the entries $A(i, j)$ of I_A (resp. $B(i)$ of I_B) that are ‘0’ mean that there are no relation (dynamical interaction) between the state x_{t+1}^i at time $t+1$ and the state x_t^j at time t (resp. the state x_{t+1}^i at time $t+1$ and the input m_t at time t). The entries that are ‘1’ mean that there is a relation. As a simple example, let us consider again the LPV system with the setting

$$A_{\rho(t)} = \begin{pmatrix} a & 0 & 1 \\ \rho^1(t) & \rho^2(t) & 0 \\ a & 1 & 1 \end{pmatrix}, \quad B = \begin{pmatrix} 1 \\ 0 \\ 0 \end{pmatrix}$$

where a is a constant element in \mathbb{F} , $\rho^1(t)$ and $\rho^2(t)$ are varying parameters in \mathbb{F} . The dynamical matrix and the input matrix I_A and I_B of the corresponding structured linear system read:

$$I_A = \begin{pmatrix} 1 & 0 & 1 \\ 1 & 1 & 0 \\ 1 & 1 & 1 \end{pmatrix}, \quad I_B = \begin{pmatrix} 1 \\ 0 \\ 0 \end{pmatrix}.$$

As a consequence, if the structural linear system (22) derived from (12) is flat, the flatness will hold for any $\rho(t)$ or equivalently any nonlinearity φ^i (any S-box will be admissible). Hence, the challenge is to define a methodology to construct flat linear structural systems. It is the purpose of the graph-based approach provided in [20] which follows the steps recalled in Appendix B. Roughly speaking, given a triplet (n, r, n_a) with n the dimension of the state, r the delay and n_a the number of non-zero entries of the matrix A , a digraph $\mathcal{G}(\Sigma_\Lambda)$ is constructed according to given rules and the matrices I_A and I_B are derived.

The triplet (n, r, n_a) , the number of non-linear functions φ^i and their locations in the matrix I_A determine a family of flat LPV-based SSSC. Next subsection aims at

summarizing the steps needed for the design of such a family. Then, a particular instantiation, leading to the SSSC called *Stanislas*, is given in next section.

1) *Summary for the construction of SSSC from a flat LPV-based automaton*: Choose a triplet (n, r, n_a) with n the dimension of the state, r the delay and n_a the number of non-zero entries of the matrix A .

Step S1: Choose a component x_t^i on which the plaintext symbol m_t is added. It follows that $B = (0 \dots 1 0 \dots 0)^t$ (the entries 1 is located at column i).

Step S2: Choose a component x_t^i ($i \in \{1, \dots, n\}$) as the desired flat output $y_t = x_t^i$. It follows that $C = (0 \dots 0 1 0 \dots 0)$ (the only entry 1 is located at the i -th column of C). It can be shown that for the special case when $B = (1 0 \dots 0)$, i must be equal to r for $y_t = x_t^i$ to be a flat output.

Step S3: Construct the corresponding digraph $\mathcal{G}(\Sigma_\Lambda)$ according to Step 1-5 given in Appendix B and derive the matrices I_A and I_B of the structured linear system Σ_Λ .

Step S4: Replace some of the non-zero entries of I_A by a nonlinear function $\rho^i(t) = \varphi^i(c_t, c_{t-1}, \dots, c_{t-s})$ to construct the matrix $A_{\rho(t)}$ of (12) and set $B = I_B$. Not all '1' entries of I_A must be assigned to a non-linear function. Some of them can be merely constant. The choice must obey a trade-off between complexity of the architecture and security (a matter discussed in next section). Since the construction ensures structural flatness, any choice will preserve the self-synchronization property.

Step S5: Complete the design by deriving the equations of Proposition 1. In particular, calculate the matrix (17) governing the state transition function of the automata (16) ensuring the deciphering.

Example: Consider the triplet $(n = 2, r = 2, n_a = 5)$. Choose

$$B = \begin{pmatrix} 1 \\ 0 \end{pmatrix}, C = (0 \ 1).$$

The particular setting of the matrix C means that the component x_t^2 of the state vector of the LPV system (12) is the desired flat output.

For $n_a = 5$, Steps 1-5 given in Appendix B give

$$I_A = \begin{pmatrix} 1 & 1 \\ 1 & 1 \end{pmatrix}, I_B = \begin{pmatrix} 1 \\ 0 \end{pmatrix}. \quad (23)$$

Let us keep constant and equal to 1 the first three entries of A and let the fourth entry be a nonlinear function. It is denoted by $\rho^1(t)$. This finally leads to the following matrix $A_{\rho(t)}$:

$$A_{\rho(t)} = \begin{pmatrix} 1 & 1 \\ 1 & \rho^1(t) \end{pmatrix}.$$

Calculate $P_{\rho(t:t+2)} = A_{\rho(t)} - B C A_{\rho(t+1)} A_{\rho(t)}$. One obtains

$$P_{\rho(t:t+2)} = \begin{pmatrix} -\rho^1(t+1) & -\rho^1(t)\rho^1(t+1) \\ 1 & \rho^1(t) \end{pmatrix}.$$

Next sections are devoted to the specifications, design rationale and security analysis of a complete SSSC based on flat LPV dynamical systems as described above. The cipher is called *Stanislas* for Secure Transmission Algorithm

with Nontriangular Iterative Structure Looking After Self-synchronization.

III. SPECIFICATION OF THE FLAT LPV-BASED SSSC STANISLAS

Stanislas operates over the 16 elements of the finite field \mathbb{F}_{16} defined as: $\mathbb{F}_{16} = \mathbb{F}_2[X]/(X^4 + X + 1)$, the addition being the componentwise exclusive or, simply denoted $+$, and the multiplication, denoted by \cdot , being the polynomial multiplication modulo the primitive polynomial $X^4 + X + 1$.

A. Equations of *Stanislas*

The internal state $x_t \in \mathbb{F}_{16}^{40}$ of the cipher consists in a vector of dimension $n = 40$ with 4-bit components considered as elements in \mathbb{F}_{16} . The input m_t and the output c_t of the ciphering function are 4-bit respective elements in \mathbb{F}_{16} . See Fig. 1 for a graphical representation of *Stanislas*.

1) *Ciphering equations*: The ciphering equation defines the next internal state $x_{t+1} \in \mathbb{F}_{16}^{40}$ and the cipher output $c_t \in \mathbb{F}_{16}$. Note also that all elements that compose the matrix $A_{\rho(t)}$ and the vectors B and C are elements of \mathbb{F}_{16} . The ciphering equation obeys, for $t \geq 0$,

$$\text{cipher: } \begin{cases} x_{t+1} &= A_{\rho(t)}x_t + Bm_t \\ c_{t+1} &= Cx_{t+1} \end{cases} \quad (24)$$

where B is the column vector equal to $B = (1_{\mathbb{F}_{16}}, 0_{\mathbb{F}_{16}}, \dots, 0_{\mathbb{F}_{16}})^T$ and C is the row vector equal to $C = (0_{\mathbb{F}_{16}}, 0_{\mathbb{F}_{16}}, 1_{\mathbb{F}_{16}}, 0_{\mathbb{F}_{16}}, \dots, 0_{\mathbb{F}_{16}})$ with the $1_{\mathbb{F}_{16}}$ component located at column $r = 3$. In other words, the only non-zero component of C which equals $1_{\mathbb{F}_{16}}$ is the third component. Hence, the ciphertext symbol consists in the third component of the internal state. Let us note that in general, the ciphertext obeys Equation (13). Hence, the ciphertext results from a linear combination of the state vector components. Here, we propose a construction for which the linear combination reduces to the selection of one component. To guarantee a self-synchronization property (otherwise stated, to ensure Equation (20)), the component that is selected must coincide with r , the delay of the system. This is why here, $r = 3$.

The matrix $A_{\rho(t)}$ is a 40×40 dimensional matrix (see Fig. 2 of Appendix). The entries a_{ij} of $A_{\rho(t)}$ are either 0 of \mathbb{F}_{16} , or 1 of \mathbb{F}_{16} or a nonlinear function of c_t . Among them, $n_a = 115$ entries are non-zero coefficients and $L = 80$ entries correspond to nonlinear functions φ^i ($i = 1, \dots, 80$). Each function φ^i depends on the current ciphertext symbol c_t ($s = 0$ in Equation (21)) and on a subkey SK_i of K . This subkey SK_i thus defines the corresponding function φ^i which depends on only one ciphertext symbol c_t as shown on Fig. 1.

$$\varphi^i: \mathbb{F}_{16} \rightarrow \mathbb{F}_{16} \\ c_t \mapsto S(c_t \oplus SK_i) \quad (25)$$

where the subkey SK_i is a 4-bit word derived from the secret key K as described in the Key Schedule of subsection III-A3 detailed further on. The function S is the bijective S-Box extracted from Piccolo [21]. It is defined on 4-bit words

by Table I. The entries a_{ij} according to their location (row i , column j for $i, j \in \{1, \dots, 40\}$) are given in Appendix A in a symbolic manner. In the symbolic representation of $A_{\rho(t)}$, denoted A_S , the functions φ^i ($i = 1, \dots, 80$) are assigned to the entries of S . Thus, the first line of the Fig. 1 corresponds to the first row of the matrix A_S applied to the internal state x_t to produce the corresponding coefficient of the internal state x_{t+1} (combined with m_t to produce c_{t+1}).

TABLE I
S-BOX IN HEXADECIMAL NOTATION.

x	0	1	2	3	4	5	6	7	8	9	A	B	C	D	E	F
$S(x)$	E	4	B	2	3	8	0	9	1	A	7	F	6	C	5	D

In other words, taking into account the particular structure of the matrices B and C with only one non-zero coefficient, the ciphering process is governed by:

$$\begin{aligned} x_{t+1}^1 &= \sum_{j=1}^n a_{1j}x_t^j + m_t \\ x_{t+1}^i &= \sum_{j=1}^n a_{ij}x_t^j, \quad i = 2, \dots, n \\ c_{t+1} &= Cx_{t+1} = x_{t+1}^3 \end{aligned} \quad (26)$$

2) *Deciphering equations:* The deciphering is governed by two equations defined, for $t \geq 0$, by

$$\text{decipherer: } \begin{cases} \hat{x}_{t+1} &= P_{\rho(t:t+r)}\hat{x}_t + B\mathcal{T}^{-1}c_{t+r} \\ \hat{m}_{t+r} &= \mathcal{T}^{-1}(c_{t+r} - C \prod_{l=t+r-1}^t A_{\rho(l)}\hat{x}_t) \end{cases} \quad (27)$$

where the 40×40 -dimensional matrix $P_{\rho(t:t+r)}$ over \mathbb{F}_{16} verifies $P_{\rho(t:t+r)} = A_{\rho(t)} - B\mathcal{T}^{-1}C \prod_{l=t+r-1}^t A_{\rho(l)}$ and $\mathcal{T} = C \prod_{l=t+r-1}^{t+1} A_{\rho(l)}B$.

Otherwise stated, the deciphering consists of two equations. The first one achieves the computation of the next internal state \hat{x}_{t+1} from the current state \hat{x}_t and the delayed ciphertext c_{t+r} . The second equation ensures the recovery of the plaintext symbol m_t . The self-synchronization between the internal states x_t and \hat{x}_t of the cipher and the decipher automata and thus a proper decryption are guaranteed, by construction, after a finite transient time.

Let $X[i]$ denotes the i -th row of a matrix X . Taking into account the particular structure of the matrices A , B and C , the delay $r = 3$, and noticing that \mathcal{T} equals one, the deciphering process is governed by:

$$\begin{aligned} \hat{x}_{t+1}^1 &= (P_{\rho(t:t+3)}[1] \cdot \hat{x}_t) + c_{t+3} \\ \hat{x}_{t+1}^i &= (P_{\rho(t:t+3)}[i] \cdot \hat{x}_t) \quad i = 2, \dots, 40 \\ \hat{m}_{t+3} &= (A_{\rho(t+2)}A_{\rho(t+1)}A_{\rho(t)})[3] \cdot \hat{x}_t + c_{t+3} \end{aligned} \quad (28)$$

where

$$\begin{aligned} P_{\rho(t:t+3)}[1] &= A_{\rho(t)}[1] - (A_{\rho(t+2)}A_{\rho(t+1)}A_{\rho(t)})[3] \\ P_{\rho(t:t+3)}[i] &= A_{\rho(t)}[i], \quad 2 \leq i \leq n. \end{aligned} \quad (29)$$

3) *Key Schedule:* The matrix A consists of $n_a = 115$ non-zero entries, and among them, $L = 80$ are functions φ^i depending on the subkey SK_i . Thus, the Key Schedule process aims at generating 80 subkeys of 4-bit length: SK_1, \dots, SK_{80} from the 80-bit master key K arranged as 20 words K_1, \dots, K_{20} of 4-bit length. To do so, the ciphering equations (26) with $m_t = 0$ are used. During this process, the parameters SK_i involved in the functions φ^i

(see Equation (25)) are set to zero. The internal state x_0 is initialized by duplicating the master key K as $(x_0^1 \dots x_0^{20}) = (K_1 \dots K_{20})$ and $(x_0^{21} \dots x_0^{40}) = (K_1 \dots K_{20})$. Then, the initial internal state x_0 is updated ten times by using equations (26) with $m_t = 0$ for $t = 0, \dots, 9$.

After those ten iterations, the ten subkeys SK_1, \dots, SK_{10} are respectively initialized with the following components of the internal state x_{10} : $x_{10}^1, x_{10}^2, x_{10}^7, x_{10}^{10}, x_{10}^{17}, x_{10}^{18}, x_{10}^{22}, x_{10}^{26}, x_{10}^{28}, x_{10}^{34}$. This process is repeated 7 more times to initialize the other subkeys $SK_{10i+1}, \dots, SK_{10i+10}$, for $i = 0, \dots, 7$.

B. Ciphering Process

The plaintext consists of ℓ elements of \mathbb{F}_{16} : $m = m_0 \dots m_{\ell-1}$. The initial state x_0 is first initialized with 40 random elements of \mathbb{F}_{16} . These initial values are kept secret and are not transmitted to the decipher even if it is possible to recover the secret key. The way those elements are randomly picked is out of the scope of this paper. Only consider that you have a source of randomness. x_0 could be considered as a secret nonce.

Then randomly pick $n - 1 = 39$ elements m_{-39}, \dots, m_{-1} of \mathbb{F}_{16} as the synchronization sequence which is placed before the plaintext. It is recalled that at most $n = 40$ iterations are needed for the self-synchronization to be achieved.

Then, because of the parameter value $r = 3$ that induces a delay, randomly pick $r - 1 = 3 - 1 = 2$ more elements $m_\ell, m_{\ell+1}$ of \mathbb{F}_{16} that will be placed at the end of the plaintext sequence m to process the two last plaintext symbols. Finally, the sequence that must feed the cipher is $m^* = m_{-39}, \dots, m_0, \dots, m_\ell, m_{\ell+1}$.

The resulting ciphertext consists of the sequence $c_{-39}, \dots, c_{\ell+1}$ of $(\ell + 41)$ symbols in \mathbb{F}_{16} , computed with the ciphering Equations (26) using Matrix A_S given in Appendix A for t in $-39, \dots, \ell + 1$:

$$\begin{aligned} x_{t+1}^1 &= S(x_t^{20} \oplus SK_0) \oplus S(x_t^{26} \oplus SK_1) \\ &\quad \oplus S(x_t^{29} \oplus SK_2) \oplus S(x_t^{40} \oplus SK_3) \oplus m_t \\ x_{t+1}^2 &= x_t^1 \oplus S(x_t^2 \oplus SK_4) \oplus S(x_t^{31} \oplus SK_5) \\ &\quad \oplus S(x_t^{35} \oplus SK_6) \\ x_{t+1}^3 &= x_t^2 \oplus S(x_t^3 \oplus SK_7) \\ x_{t+1}^4 &= S(x_t^2 \oplus SK_8) \oplus S(x_t^3 \oplus SK_9) \\ &\quad \vdots \\ c_{t+1} &= x_{t+1}^3 \end{aligned}$$

Those equations are the ones given in Fig. 1 corresponding with the coefficients of the Matrix A_S .

Note that the Matrix A_S given in Appendix A could be seen as one round of a block cipher applied on a state with 40 many 4-bit words where after each round the 4-bit word x^3 is outputted whereas the 4-bit word x^0 is completely updated by other 4-bit words. At each clock, each 4-bit word crosses at least one S-box, except the 4-bit word x^1 that could be considered as a temporary variable (as it receives the 4-bit message m_t). Note also that the updated rule for most of the variables x^i ($5 \leq i \leq 40$) could be written as $x_{t+1}^i = S(x_t^{i-1} \oplus SK_k) \oplus f(x_t^{i-2})$ or

$S(x_t^{i-1} \oplus SK_k) \oplus f(x_t^{i-2}) \oplus S(x_t^j \oplus SK_{k'})$ for given j, k and k' and where f is the identity or the S-box S . It could be seen as a generalization of the so-called L -scheme with a circular permutation used in the block cipher MISTY1 with balanced inputs/outputs. The complete ciphering process of Stanislas is illustrated on Fig. 1.

C. Deciphering Process

The decipherer receives the cryptogram consisting of $\ell + 41$ symbols $c_{-39}, \dots, c_{\ell+1}$ in \mathbb{F}_{16} . The internal state \hat{x}_0 is initialized to an arbitrary value, for example the zero value.

Then, the deciphering Equations (28)-(29) are applied to recover a $\ell + 41$ -length message $\hat{m} = \hat{m}_{-41}, \dots, \hat{m}_{\ell-1}$. The plaintext sequence is recovered as the last ℓ symbols $m = \hat{m}_0 \dots \hat{m}_{\ell-1}$.

Remark 2: It could be surprising that a part of the ciphering process directly depends on a secret nonce (i.e. x_0). Instead, we could imagine that an 80-bit IV is used to generate the first value x_0 adding an IV schedule to the Key Schedule process. First, generate the subkeys using the Key Schedule, then initialize the internal state with the concatenation of the IV and of the key. Then, apply again the Key Schedule process (but including the generated subkeys SK_i in the S-boxes) to initialize the internal state x_0 . But, note that in this case, the particular property that the internal states (that must be kept secret) of the ciphering part and of the deciphering part are not required to be equal is lost. Indeed, in this case where an IV is used, we will suppose that the internal state will be computed in the same way in both sides.

The matrix A consists of $n_a = 115$ non-zero entries, and among them, $L = 80$ are functions φ^i depending on the subkey SK_i . Thus, the Key Schedule process aims at generating 80 subkeys of 4-bit length: SK_1, \dots, SK_{80} from the 80-bit master key K arranged as 20 words K_1, \dots, K_{20} of 4-bit length. To do so, the ciphering equations (26) with $m_t = 0$ are used. During this process, the parameters SK_i involved in the functions φ^i (see Equation (25)) are set to zero. The internal state x_0 is initialized by duplicating the master key K as $(x_0^1 \dots x_0^{20}) = (K_1 \dots K_{20})$ and $(x_0^{21} \dots x_0^{40}) = (K_1 \dots K_{20})$. Then, the initial internal state x_0 is updated ten times by using equations (26) with $m_t = 0$ for $t = 0, \dots, 9$.

IV. DESIGN RATIONALE AND SECURITY ANALYSIS

In this section, we motivate the choices of the field on which the cryptosystem operates, the dimension n of the internal state, the delay r and the structure of the matrix A . Most of the choices rest on security criteria, other ones take into account practical considerations, regarding in particular the hardware implementation issues.

A. Design Rationale

a) Field on which the cryptosystem operates: Galois field $GF(16)$: Any quantities m_t, c_t , components of x_t and \hat{x}_t and non-linear functions φ^i (S-boxes) inputs are 4-bit data. It is motivated by the fact that the cryptosystem is

intended to be implemented on a digital equipment. Hence, field extensions and so, power of two are required. On the other hand, 8-bit would be too heavy for an embedded algorithm. In particular, S-boxes would involve too many logic gates.

b) Dimension $n: 40$: As the internal state components are 4-bit words, a dimension $n = 40$ provides an internal state of 160 bits and thus a security level of 80 bits. Indeed, to prevent time-memory trade-off attack [22] (an attack which is a trade-off between exhaustive search and table look-up), the internal state must be two times longer than the key length which defines the security level. This level is compatible with a real-world application.

c) Delay $r: 3$: The more the delay, the more the algebraic degree of the entries of $P_{\rho(t:t+r)}$, recalling that $P_{\rho(t:t+r)}$ involves the product of r matrices (see (29)). Thus, for a good resistance against an algebraic attack ([23]), the algebraic degree should be as large as possible. On the other hand, the more the delay, the more the complexity of implementation and the less the computational performances. The delay $r = 3$ results from a trade-off between security with respect to algebraic attacks (to increase the overall algebraic degree) and ease of implementation (especially the implementation of the P deciphering matrix which involves several S-box multiplications (see Equation (17) in the general case and (29) for Stanislas)).

d) Structure of the matrices A and P : We recall that the matrix A (and thus P from the computation (29)) is derived from the construction of a digraph (see Appendix B) from which an adjacency matrix I_A is extracted. More precisely, the adjacency matrix I_A determines the entries of $A_{\rho(t)}$ that are zero and the others that are possibly non-zero. The number n_a of edges in the digraph $\mathcal{G}(\Sigma_A)$ corresponds to the number of non-zero entries of I_A . Hence, the number n_a also determines the number of non-zero entries of the state transition matrix P . Beyond the number of non-zero entries, their location (row and column) must also be chosen. Finally, it must be decided whether a non-zero entry will be 1 or will correspond to an S-box. All those issues have been addressed by considering several criteria regarding the security, in particular the good resistance to classical attacks and the good diffusion delay, while satisfying a trade-off with respect to the computational complexity for the sake of implementation. Let us introduce symbolic representations of $A_{\rho(t)}$ and $P_{\rho(t)}$ denoted by A_S and P_S where the coefficients of A_S and P_S belong to $\mathbb{Z}[S]$, S representing any non-linear function. The following considerations on A_S and P_S can be made.

Diffusion Delay and Depth. The diffusion delay and the depth are properties related to the consideration of the powers A_S^p and of P_S^p as p , a natural integer, increases. Indeed, the power of matrices results from the successive iterations of the ciphering and the deciphering process. Let p denotes the power of a matrix $Z \in M_n(GF(16))$. The diffusion delay, introduced in [14], is the smallest value, denoted by d_0 , of p such that Z^p does not have any zero coefficient. In other words, it is the smallest value of p such that each element of the initial internal state x_0

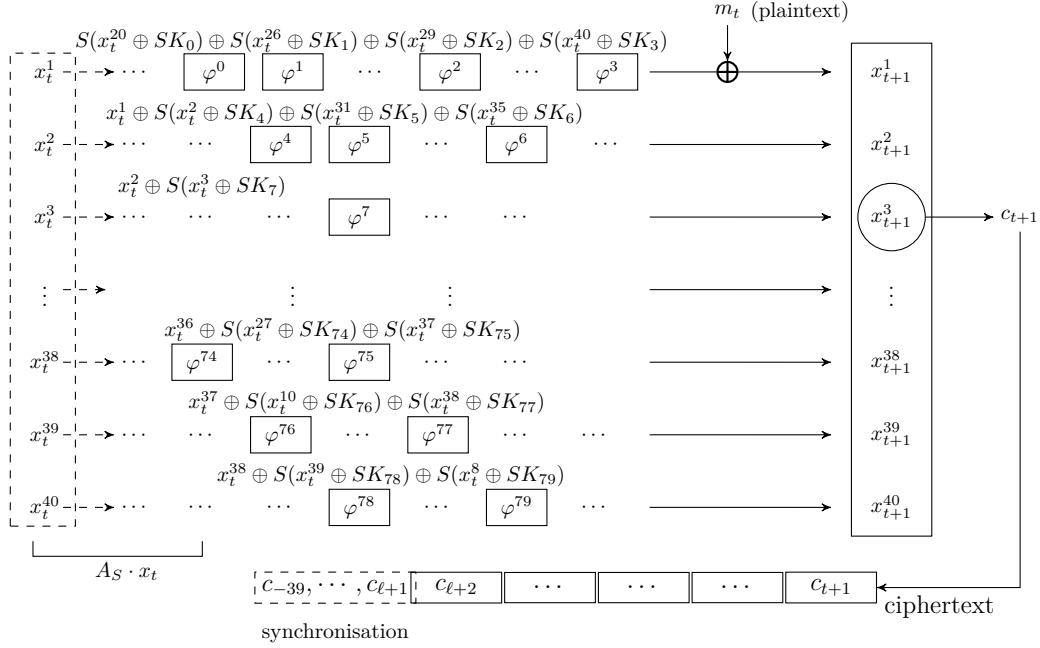


Fig. 1. The complete ciphering process of Stanislas with $\varphi^i(x_t^j) = S(x_t^j \oplus SK_i)$. x_t^i and x_{t+1}^i are the coefficients of the internal state at time t and time $t+1$. m_t represents a plaintext symbol (4 bits), c_j the ciphertext symbols (4 bits) where c_{-39}, \dots, c_{t+2} are required for synchronisation. The equations of the lines are derived from the coefficients of the rows of the Matrix A_S .

has influenced every element of x_t for $t \geq d_0$. The depth, introduced in [24], is the smallest value, denoted by d_1 , of p such that any entry of Z^p are polynomials of degree at least 1. We are looking for the smallest values of d_0 and d_1 .

Algebraic Degree. Considering the matrix resulting from successive powers of A_S and P_S , we are first interested in ensuring that at least one entry has the largest algebraic degree. To this end, we must add a cycle on the r -th vertex of the digraph $\mathcal{G}(\Sigma_\Lambda)$, which equivalently means that the entry of A_S and P_S located at row r and column r must be an S-box. Furthermore, the evolution of this quantity, after successive iterations, must meet an ideal shape: it must increase by one at each iteration, must remain constant and equal to its maximum value as long as possible and finally must drop down to zero (let us recall that after 40 iterations, due to (20), the product reaches exactly zero).

Full-Rank Matrix. The fact that A_S is a full-rank matrix is a necessary condition to ensure a full diffusion of the internal state and to maximize the dependency between the involved terms at time t and the involved terms at time $t+1$. Moreover, this condition guarantees that the encryption process does not collapse. By construction (see Appendix B) to ensure flatness, every element of the subdiagonal of I_A from the r -th one is 1. Hence, for A_S to be full-rank, each column and each row must contain at least one non-zero element. And yet, by construction, only the $r-1$ first elements of the last column can be non-zero. Hence, one of them must be non-zero. From the digraph point of view, it means that at least one of the $r-1$ first vertices must be connected to the last vertex.

The symbolic matrix A_S which has been finally selected is given in Appendix A. It has been obtained after

700000 random runs performed under the aforementioned constraints: best diffusion delay and depth, algebraic degree (especially increase by 1 at each iteration), full-rank matrix. Several matrices correspond to the best choices (we add a sum indicator without weighing) and we finally chose the one with the best implementations for A_S and for P_S . The symbolic matrix P_S can be directly obtained by considering Equations (29). The matrix A_S involves $n_a = 120$ non-zero entries and its number of S-boxes is $L = 80$. The matrix extracted from A_S and P_S by removing the first r rows and columns have a special feature. The lower subdiagonal is full of coefficients S (corresponding to S-boxes and denoted SB in the symbolic representation) and the subsubdiagonal just above is full of 1. Thus, each line has at least one S-box to ensure that the internal state x_t is updated in a non-linear way: this corresponds to a non-linear shift register.

The corresponding diffusion delay, $d_0 = 7$, could be considered as a good diffusion delay with regard to the synchronization delay that equals 40 (the system dimension). Indeed, the worst diffusion delay is equal to 40 and the best diffusion delay of 1 could only be reached with a matrix full of non-zero coefficients. Thus, we consider that a diffusion delay of 7 is a sufficiently good compromise between the best diffusion delay and a reasonable number of non-zero coefficients.

Let us notice that the dimension n of the system is the upper bound of the diffusion delay. Indeed, due to (20), the product reaches exactly zero in $GF(16)$ since the synchronization is achieved after at most 40 iterations. The depth is $d_1 = 7$ and is the best that we manage to achieve.

e) S-box: Various classifications of 4-bit S-boxes exist in the literature [25], [26], [27]. For the sake of hardware

optimization, the same S-box has been used to define the $L = 80$ nonlinear functions φ^i . Two kinds of criteria have been considered: theoretical and practical. On one hand, we have selected S-boxes to satisfy the maximum differential probability and the maximum (absolute) linear bias 2^{-2} , the algebraic degree 3, and no fixed-point. Four S-boxes that satisfy those criteria and that have simple algebraic expressions (i.e. a minimal number of non-linear transformations) have been selected, each one corresponding respectively to the four classes proposed in [27].

From an implementation point of view, it turns out that the S-box depicted in Table I induces the smallest gate count. It is the Piccolo S-box ([21]). The area is around 23 Gate Equivalents (GEs)¹. It involves four NOR gates, three XOR gates and one XNOR gate. Let us notice that the masking method can be applied using only three shares, making this S-box suitable for efficient threshold (i.e. side-channel protected) implementations.

f) *Key Schedule*: The Key Schedule has been chosen to reuse existing circuit while sufficiently mixing together the key words. To do so, we use the already implemented matrix A by applying it a sufficient number of times when looking at the diffusion degree and at the induced algebraic degree. The extracted 4-bit words of the internal state x_t - at positions 1, 2, 7, 10, 17, 18, 22, 26, 28, 34 - have been chosen to be among the ones that depend of the maximum number of other elements of x_t to ensure to maximize the diffusion effect of the initial state x_0 .

From a theoretical point of view, if we consider that each S-box behaves as a random function (i.e. it has a behavior sufficiently near the one of a true random function) and using the direct extension of Lemma 9 and Theorem 7 of [28], we could say, that after $d_0 + 2$ of the matrix A on the input x_0 , the applied transformation behaves as a random function. In other words, the operations done to fulfill the subkey words behaves as a random function.

B. Security Analysis

The following section focuses on the security of *Stanislas* against known attacks. We claim a 80-bit security level which corresponds to the key length (we could not have a security level greater than the key length). Moreover, this security level is also achieved regarding the length of the main register: 160 bits. Indeed, the Guess-and-Determine attacks described in [22] imply to double the length of the used register compared to the key length to achieve a security level corresponding to the key length. Thus, we try to derive security bounds for all known attacks against *Stanislas* and we found no attacks that work with a complexity smaller than 2^{80} operations which corresponds with our security claim.

Moreover, it has been proven in [29] that the canonical form of an SSSC is secure against Chosen Plaintext Attacks (IND-CPA secure) but not against Chosen Ciphertext Attacks (IND-CCA security). We do not claim any security

result in this last model. Moreover, we suppose that the attacker has no access to the key and to the initial value of the internal state x_0 . To prevent collision search attack, we limit the size of each plaintext to 2^{64} 4-bit words.

First, it seems very difficult to analyze the security of *Stanislas* in its true settings (i.e. the 160-bit internal state x_0 is a secret nonce). In those settings, we could only say that:

- the time-memory-data trade-off attacks described in [30], [31], [22] apply when the internal state is smaller than two times the key length. This is why we choose the length of the internal state to be twice the key length to prevent this kind of attacks.
- Guess-and-Determine Attacks [22] consist in guessing a part of the state to further determine the remaining part of the state. Thus, at time t , suppose that we know x_t^2, x_t^3 and of course, c_t . Thus, we could suppose that we observe n consecutive outputs from c_t to c_{t+n} . Thus, how much does it cost to recover the induced subkey SK_i ? First, from the equation $x_{t+1}^3 = x_t^2 \oplus S(x_t^3 \oplus SK_7)$, we could directly compute SK_7 . Thus, we could derive the successive value of x_t^2 from t to n . Thus, from x_t^2 we derive non-linear equations where the unknowns are $x_t^1, x_t^{31}, x_t^{35}, SK_5, SK_4$ and SK_6 and the known terms are x_t^2 to x_{t+n}^2 . Thus, as the Algebraic Normal Form (ANF) of the S-box has 2 equations with 4 terms, 1 equation with 9 terms and 1 equation with 7 terms, each new x_t^2 will induce a system of $4 \times 3 \times (n + 1) + 3 \times 4 = 12n + 24$ unknown binary variables with 4 equations with in total 24 non-linear terms. Thus, we could not solve the system without guessing a part of it whatever the n value. Even considering that we guess a part of the system, the combinatorial explosion seems clear because each value of the internal state depend on at least one other value. Thus, we conjecture here that *Stanislas* is safe against this type of attacks since, even if a part of the internal state is guessed, each 4-bit word of this state is updated through a XOR with a 4-bit word of subkey and an S-box. Moreover, since the diffusion delay of A_S is $d_0 = 7$, this leads to guess after 7 outputs all the key. Thus, guessing a part of the state allows to guess a part of the key which, in then, amounts to a guess-and-determine attack with a complexity greater than the key exhaustive search.

Thus, instead, when looking at classical attacks, we will use the model described in Remark 2 where the initial state is derived in its first components after 20 iterations of the matrix A_S applied on the concatenation of an IV and of the master key K and in its last components after 14 more iterations. Those settings could be considered as a degrading mode of the original *Stanislas* specifications. Thus considering that the attacker has full access to the IV, we obtain the following bounds against classical attacks.

Differential / Linear Cryptanalysis: we compute the lower bounds on the minimal number of active S-boxes for the computation of the internal state with Remark 2.

¹Section V describes the meaning of GE metric.

To do so, we implement the model of Remark 2 using Constraint Programming to explore all the possible paths in the induced graph. Then, we obtain that, for the differential case, after 7 iterations, a minimal number of 38 S-boxes has been crossed, after 10 iterations, 46, after 14 iterations, 65. As the differential probability of the chosen S-box is equal to 2^{-2} , we could guarantee that the 80-bit key exhaustive search is less expensive than passing through more than 40 S-boxes, which is the case after 10 iterations of the A_S matrix. In the same way, for the linear case, we obtain after 7 iterations, 35 active S-boxes, after 10 iterations, 41 and after 14 iterations, 59. Thus, for the same reason, after 10 iterations, a 80-bit key exhaustive search is more efficient.

Algebraic Attacks: This kind of attacks [23] is possible when the overall degree of the induced system of equations does not sufficiently increase at each clock. Especially, if the overall degree d in each of the n unknown variables (the key variables for example) of the system is such that $(n^d)^{2.5}$ is lower than the security bounds, it means that it is faster to solve the induced system by Gaussian elimination (considering that each new monomial is a new unknown variable) than trying all the keys of the system. Thus, we want to prevent this attack from happening as described below. The algebraic degree of each S-box component is the best one: equal to 3. Thus, each passing through an S-box increases the degree in the equations describing the internal state and in the equations describing the key. Even if the SK_i linearly depends on the master key bits K_1, \dots, K_{80} (there are 80 key bits that are unknown), if we write the number of variables after crossing the first S-box, we have $(80)^3$ monomials depending on the unknown key bits, after the second pass we obtain $(80)^6$ monomials also depending on the unknown key bits and so on. Thus, if we apply those estimations using the bounds on the number of active S-boxes of the differential/linear case, after 10 iterations, we have 46 active S-boxes, which means that the number of unknowns (considering that each new monomial is a new unknown) is lower bounded after 10 iterations by $(80)^{3 \times 46} \approx 2^{872.16}$ where 80 are the unknowns coming from the master key, 3 is the algebraic degree of the S-box and 46 is the number of crossed S-boxes. Thus, we conjecture that the complexity of the best algebraic attack is greater than the 80-bit key exhaustive search.

Cube Attacks: As established in [32], a cipher is vulnerable to cube attacks if an output bit can be represented as a sufficiently low degree polynomial over $GF(2)$ of key and input bits. It works by summing an output bit value for all possible values of a subset of public input bits, chosen such that the resulting sum is a linear combination of secret bits. Repeated application of this technique gives a set of linear relations between secret bits that can be solved to discover these bits. In [33], the authors analyzed this kind of attacks on the block cipher Piccolo, especially its S-box. They stated that after 8 rounds, no relation with 63 input bits could be found. The minimal number of S-boxes crossed for 8 Piccolo rounds is 58 whereas in our case, it is 46 after 10 iterations. So we conjecture that we cross a sufficient number of S-boxes after few iterations to prevent

having low degree relations between secret key bits and public input bits.

In summary, we conjecture that most of the usual attacks which apply in the stream cipher context have a complexity greater than the exhaustive key search for Stanislas.

V. HARDWARE PERFORMANCE AND IMPLEMENTATION ASPECTS

We give hereafter the implementation results of a straightforward implementation of Stanislas. It produces one 4-bit word of ciphertext per clock cycle. Subkeys are computed in the initialization step using the Key Schedule and stored in dedicated registers, before the cipher state processing. The same material is used for the cipher state and the Key Schedule processes. The hardware implementation of Stanislas is not an optimized version targeting any specific performance. The main area occupation comes from the matrix update as it carries big registers during all the calculations. Those registers are the internal state which are mixed with the subkeys either with binary addition or multiplication. This means updating a 40×4 bits register all along the matrix update. During ciphering process, the matrix update is solely made of S-boxes and XOR of 4-bit words. The lowest line of the matrix in terms of area occupation is made of 1 S-box and 2 additional XORs, the biggest of 4 S-boxes and 8 additional XORs. The deciphering process implies adding 23 multiplications, 28 S-boxes and 39 XORs to the previous total which makes deciphering heavier in terms of area occupation. The matrix is implemented line by line, calculated straightforwardly following the equations as depicted in Fig. 1. The S-boxes are implemented in a Look-Up-Table (LUT) way, so we let the compiler do its own optimizations. Our Stanislas implementation combines both the encryption and decryption process in order to ease comparisons with other (synchronous or self-synchronizing) stream ciphers.

We implemented Stanislas in VHDL and we provide in Table II FPGA hardware implementations and performance comparisons with synchronous SCs TRIVIUM [17] and Grain [18], final members of the eSTREAM portfolio, another SSSC Moustique and the AES-based SSSC CFB1-AES128 as defined in NIST SP 800-38a [12]. The chosen FPGA platform for our benchmark is the Xilinx Spartan-6 XC6SLX75T, package FGG676. High effort of the Xilinx ISE Design Suite has been put on area reduction. Post-place-and-route results are provided.

To get TRIVIUM, Grain, Moustique and CFB1-AES128 implementation results, we have designed our own VHDL straightforward reference implementations, without further optimization in mind. For this latter, we have implemented the potential S-boxes as LUTs, to be consistent with the S-boxes LUT implementations of Stanislas.

At first sight, we can check that some well-known properties are visible in the results. For example, TRIVIUM and Grain are very compact, which can be explained by their low combinatorial gate counts. Moreover, the number of initialization cycles needed for TRIVIUM, Grain

	Area (slices)	Init. (cycles)	Synchro. (cycles)	Freq. (MHz)	TP (Mbps)
TRIVIUM	47	1603	0	191	191
Grain	48	256	0	355	355
MOUSTIQUE	166	105	105	309	309
CFB1-AES128	745	0	128	73	849
Stanislas	701	66	40	95	380

TABLE II
XILINX SPARTAN-6 XC6SLX75T (FPGA) STRAIGHTFORWARD IMPLEMENTATION RESULTS.

and Moustique is consistent with the specifications: e.g., TRIVIUM needs a warm-up phase of minimum 1152 steps. This number is really low for Stanislas where it just consists in a Key Schedule and it is equal to 0 for CFB1-AES128 where the key is processed on the fly.

Surprisingly, straightforward implementation of Stanislas provides the best throughput (TP) compared to the other stream ciphers, even self-synchronizing. The reason is that one 4-bit word is processed by clock cycle, so the throughput is given by: 95×4 (bits) = 380 Mbps. That justifies our design choice of processing 4-bit words instead of individual bits. Compared to the standard approach CFB1-AES128, the time needed for synchronization is also shorter, along with a smaller area.

This encouraging result has to be mitigated if we consider the combined metric TP/Area as shown on Table III. This latter allows to estimate the cost of optimized parallel implementations, where many bits can be processed in parallel, at the expense of additional area.

	TP/Area (Mbps/slice)
TRIVIUM	4.06
Grain	7.39
MOUSTIQUE	1.86
CFB1-AES128	1.13
Stanislas	0.54

TABLE III
COMBINED METRIC TP/AREA (Mbps/SLICE ON XILINX SPARTAN-6 XC6SLX75T FPGA).

As we can see, due to its lowest TP/Area value, straightforward implementation of Stanislas will suffer from the comparisons of its competitors' optimized versions. We can then estimate, in Table IV, the upper bounds of theoretical implementation results of all Stanislas competitors when all of them are unrolled versions which process 4 bits per clock cycle, as Stanislas.

	Area (slices)	TP (Mbps)
TRIVIUM	188	764
Grain	192	1420
MOUSTIQUE	664	1236
CFB4-AES128	2980	3396
Stanislas	701	380

TABLE IV
THEORETICAL IMPLEMENTATION RESULTS OF SOME (SS)SCS ON XILINX SPARTAN-6 XC6SLX75T FPGA FOR 4-BIT VERSIONS

As we can see, CFB4-AES128 mode has a 4-fold throughput speedup, beating Stanislas proposal with a significant margin, and it requires only 32 steps for synchronization. But it implies to occupy a big amount of FPGA slices, which is not always affordable for some constrained applications.

Future works will include the study of the cost of side-channel protected Stanislas implementations.

VI. CONCLUSION

An instantiation, called Stanislas, of a dedicated Self-Synchronizing Stream Ciphers (SSSC) has been proposed. Its main peculiarity comes from the fact that it involves an automaton with finite input memory using non-triangular state transition functions. The construction is based on a general and systematic methodology that uses automata (called Linear Parameter Varying, LPV) admitting a matrix representation and a special property called flatness. The security analysis allows to conjecture that most of the usual attacks which apply in the stream cipher context have a complexity greater than the key exhaustive search for Stanislas. But, Stanislas could not be considered having a small hardware footprint.

However, when straightforward implementations are considered, Stanislas provides bigger throughput than the considered stream ciphers, and its intrinsic synchronization delay is much smaller than the SSSC Moustique (40 clock cycles instead of 105) and the standard approach CFB1-AES128 (40 clock cycles instead of 128).

Moreover, the number of surviving Self-Synchronizing Stream Ciphers after a phase of public cryptanalysis time is equal to zero. So, we hope that Stanislas will be the first one and we encourage the symmetric key cryptographic community to cryptanalyze it.

REFERENCES

- [1] U. M. Maurer, "New approaches to the design of self-synchronizing stream ciphers," in *Advances in Cryptology - EUROCRYPT '91*, ser. Lecture Notes in Computer Science, vol. 547. Springer, 1991, pp. 458–471.
- [2] R. A. Rueppel, *Analysis and design of stream ciphers*. Springer Science & Business Media, 2012.
- [3] J. Daemen, R. Govaerts, and J. Vandewalle, "On the design of high speed self-synchronizing stream ciphers," in *Proc. of the ICCS/ISITA '92 conference*, vol. 1, Singapore, November 1992, pp. 279–283.
- [4] P. Hawkes, M. Paddon, G. G. Rose, and W. V. Miriam, "Primitive specification for sss," e-Stream Project, Tech. Rep., 2004, available at: <http://www.ecrypt.eu.org/stream/ciphers/sss/sss.pdf>.
- [5] P. Sarkar, "Hiji-Bij-Bij: A New Stream Cipher with a Self-Synchronizing Mode of Operation," 2003.
- [6] J. Daemen and P. Kitsos, "The self-synchronizing stream cipher moustique," in *New Stream Cipher Designs - The eSTREAM Finalists*, ser. Lecture Notes in Computer Science. Springer, 2008, vol. 4986, pp. 210–223.
- [7] A. Joux and F. Muller, "Loosening the KNOT," in *Fast Software Encryption - FSE 2003*, ser. Lecture Notes in Computer Science, vol. 2887. Springer, 2003, pp. 87–99.
- [8] —, "Two attacks against the HBB stream cipher," in *Fast Software Encryption - FSE 2005*, ser. Lecture Notes in Computer Science, vol. 3557. Springer, 2005, pp. 330–341.
- [9] —, "Chosen-ciphertext attacks against MOSQUITO," in *Fast Software Encryption - FSE 2006*, ser. Lecture Notes in Computer Science, vol. 4047. Springer, 2006, pp. 390–404.
- [10] E. Käseper, V. Rijmen, T. E. Björstad, C. Rechberger, M. J. B. Robshaw, and G. Sekar, "Correlated keystreams in moustique," in *Progress in Cryptology - AFRICACRYPT 2008*, ser. Lecture Notes in Computer Science, vol. 5023. Springer, 2008, pp. 246–257.
- [11] V. Klíma, "Cryptanalysis of hiji-bij-bij (HBB)," IACR Cryptology ePrint Archive, Report 2005/3, 2005.
- [12] M. Dworkin, "Nist special publication 800-38a, recommendation for block cipher modes of operation-methods and techniques," *National Institute of Standards and Technology/US Department of Commerce*, 2001. [Online]. Available: <https://csrc.nist.gov/publications/detail/sp/800-38a/final>

- [13] F. Arnault, T. P. Berger, C. Lauradoux, M. Minier, and B. Pousse, "A new approach for fcsrs," in *Selected Areas in Cryptography - SAC 2009*, ser. Lecture Notes in Computer Science, vol. 5867. Springer, 2009, pp. 433–448.
- [14] F. Arnault, T. P. Berger, M. Minier, and B. Pousse, "Revisiting lfsrs for cryptographic applications," *IEEE Trans. Information Theory*, vol. 57, no. 12, pp. 8095–8113, 2011.
- [15] B. Dravie, P. Guillot, and G. Millérioux, "Design of self-synchronizing stream ciphers: A new control-theoretical paradigm," in *IFAC World Congress, (IFAC 2017)*, Toulouse, France, July 2017.
- [16] J. Daemen and P. Kitsos, "The Self-Synchronizing Stream Cipher MOSQUITO: eSTREAM Documentation, Version 2," *eSTREAM, ECRYPT Stream Cipher Project, Report 2005/018*, 2005, available online at <http://www.ecrypt.eu.org/stream/p3ciphers/mosquito/mosquito.pdf>.
- [17] C. D. Cannière and B. Preneel, "Trivium," in *New Stream Cipher Designs - The eSTREAM Finalists*, ser. Lecture Notes in Computer Science. Springer, 2008, vol. 4986, pp. 244–266.
- [18] M. Hell, T. Johansson, A. Maximov, and W. Meier, "The grain family of stream ciphers," in *New Stream Cipher Designs - The eSTREAM Finalists*, ser. Lecture Notes in Computer Science. Springer, 2008, vol. 4986, pp. 179–190.
- [19] E. Kasper, V. Rijmen, E. Bjorstad, C. Rechberger, M. Robshaw, and G. Sekar, "Correlated Keystreams in MOUSTIQUE," ESTREAM Project, Tech. Rep., 2004.
- [20] G. Millerioux and T. Boukhobza, "Characterization of flat outputs for LPV discrete-time systems: A graph-oriented approach," in *54th IEEE Conference on Decision and Control, CDC 2015*. IEEE, 2015, pp. 759–764.
- [21] K. Shibutani, T. Isobe, H. Hiwatari, A. Mitsuda, T. Akishita, and T. Shirai, "Piccolo: An ultra-lightweight blockcipher," in *Cryptographic Hardware and Embedded Systems - CHES 2011*, ser. Lecture Notes in Computer Science, vol. 6917. Springer, 2011, pp. 342–357.
- [22] M. E. Hellman, "A cryptanalytic time-memory trade-off," *IEEE Trans. Information Theory*, vol. 26, no. 4, pp. 401–406, 1980.
- [23] N. Courtois, A. Klimov, J. Patarin, and A. Shamir, "Efficient algorithms for solving overdefined systems of multivariate polynomial equations," in *Advances in Cryptology - EUROCRYPT 2000*, ser. Lecture Notes in Computer Science, vol. 1807. Springer, 2000, pp. 392–407.
- [24] T. P. Berger and M. Minier, "Some results using the matrix methods on impossible, integral and zero-correlation distinguishers for feistel-like ciphers," in *Progress in Cryptology - INDOCRYPT 2015*, ser. Lecture Notes in Computer Science, vol. 9462. Springer, 2015, pp. 180–197.
- [25] C. D. Cannière, "Analysis and Design of Symmetric Encryption Algorithms," Ph.D. dissertation, Katholieke Universiteit Leuven, 2007.
- [26] G. Leander and A. Poschmann, "On the classification of 4 bit s-boxes," in *Arithmetic of Finite Fields, First International Workshop, WAIFI 2007*, ser. Lecture Notes in Computer Science, vol. 4547. Springer, 2007, pp. 159–176.
- [27] M.-J. O. Saarinen, "Cryptographic Analysis of All 4 x 4 - Bit S-Boxes," IACR Cryptology ePrint Archive, Report 2011/218, 2005.
- [28] U. M. Maurer, "Indistinguishability of random systems," in *Advances in Cryptology - EUROCRYPT 2002*, ser. Lecture Notes in Computer Science, vol. 2332. Springer, 2002, pp. 110–132.
- [29] B. Dravie, P. Guillot, and G. Millérioux, "Security proof of the canonical form of self-synchronizing stream ciphers," *Des. Codes Cryptography*, vol. 82, no. 1-2, pp. 377–388, 2017.
- [30] S. Babbage, "A Space/Time Trade-Off in Exhaustive Search Attacks on Stream Ciphers," in *European Convention on Security and Detection*, no. 408. IEEE Conference Publication, 1995.
- [31] A. Biryukov and A. Shamir, "Cryptanalytic time/memory/data tradeoffs for stream ciphers," in *Advances in Cryptology - ASIACRYPT 2000*, ser. Lecture Notes in Computer Science, vol. 1976. Springer, 2000, pp. 1–13.
- [32] I. Dinur and A. Shamir, "Cube attacks on tweakable black box polynomials," in *Advances in Cryptology - EUROCRYPT 2009*, ser. Lecture Notes in Computer Science, vol. 5479. Springer, 2009, pp. 278–299.
- [33] H. Sato, M. Mimura, and H. Tanaka, "Analysis of division property using milp method for lightweight blockcipher piccolo,"

in *2019 14th Asia Joint Conference on Information Security (AsiaJCIS)*, 2019, pp. 48–55.

- [34] A. Casamayou, N. Cohen, G. Connan, T. Dumont, L. Fousse, F. Maltey, M. Meulien, M. Mezzarobba, C. Pernet, N. Thiéry et al., *Calcul mathématique avec Sage*. available online: <https://hal.inria.fr/inria-00540485v2/document>, 2013.



Julien Francq received the Ph.D. degree in Computer Science domain in 2009 from the Université de Montpellier (France). He is now working in Naval Group company as a cryptography, data science and hardware security expert in the Naval Cyber Laboratory. One of his main research interests is the security and the efficiency of (hardware/software) implementations of cryptography against (mathematical/physical) attacks.



Loïc Besson started working in Airbus Cyber-Security company in 2017. In 2018, he started his Ph.D. in implementations of symmetric cryptography primitives in the company Hensoldt France.



Paul Huynh has started his Ph.D. at Université de Lorraine in 2017. He works on lightweight cryptography.



Philippe Guillot received the Ph.D. degree in 1999, from the Université de Caen. He is an Assistant Professor at Université Paris 8 and he is interested in symmetric cryptography and their hardware implementations.



Gilles Millerioux received his Ph.D. from INSA Toulouse in 1997 and his French Habilitation in 2004 from Université Henri Poincaré - Nancy 1. Between 1998 and 2005 he has been Associate professor at Université Henri Poincaré - Nancy 1. Since 2005, he is Professor at Polytech Nancy and at the Centre de Recherche en Automatique de Nancy (CRAN). His main research interest concerns control theory and its application to cryptography.



Marine Minier received the Ph.D. degree in 2002, from the Université de Limoges and the French Habilitation from the Université de Lyon in 2012. In 2005, she joined the INSA de Lyon and the CITI Laboratory, as an Assistant Professor. Since 2016, she is professor at Université de Lorraine and at the LORIA Lab. Her research interests include Symmetric Key Cryptography and Security in WSNs.

APPENDIX A
THE MATRIX A_S

The matrix A_S is given in Fig. 2.

APPENDIX B
CONSTRUCTION OF THE MATRICES OF THE SSSC

A digraph $\mathcal{G}(\Sigma_\Lambda)$ describing the structured linear system associated to the state equations (12), is the combination of a vertex set \mathcal{V} and an edge set \mathcal{E} . The vertices represent the states and the input components of Σ_Λ while the edges describe the dynamic relations between these variables. One has $\mathcal{V} = \mathbf{X} \cup \{\mathbf{m}\}$ where \mathbf{X} is the set of state vertices defined as $\mathbf{X} = \{\mathbf{x}^1, \dots, \mathbf{x}^n\}$ and \mathbf{m} is the input vertex. The edge set is $\mathcal{E} = \mathcal{E}_A \cup \mathcal{E}_B$, with $\mathcal{E}_A = \{(\mathbf{x}^i, \mathbf{x}^j) | A(i, j) \neq 0\}$ and $\mathcal{E}_B = \{(\mathbf{m}, \mathbf{x}^i) | B(i) \neq 0\}$. The entries of $A_{\rho(t)}$ correspond to the weights of the edges in the digraph. For convenience, we will denote by \mathbf{v}^j , ($j = 0, \dots, n$) a vertex of the digraph $\mathcal{G}(\Sigma_\Lambda)$ regardless of whether it is the input or a state vertex.

Given a triplet (n, r, n_a) with n the dimension of the state, r the delay and n_a the number of non-zero entries of the matrix A , the construction of the digraph $\mathcal{G}(\Sigma_\Lambda)$ related to the system Σ_Λ involves the following steps.

The system Σ_Λ is of dimension n and thus, the digraph $\mathcal{G}(\Sigma_\Lambda)$ involves $n + 1$ vertices. The input is assigned to the vertex denoted by \mathbf{v}^0 . The other n vertices are denoted by $\mathbf{v}^1, \dots, \mathbf{v}^n$. Let \mathbf{v}^r be the vertex that corresponds to the flat output \mathbf{v}^r .

Step 1: For, $i = 0, \dots, n - 1$, add the edges $(\mathbf{v}^i, \mathbf{v}^{i+1})$. There are r edges which connect \mathbf{v}^0 to \mathbf{v}^r . Hence, the delay of the automaton is r .

After Step 1, this line topology corresponds to quite trivial dynamical systems since it corresponds to state transition functions in the form of simple shifts. Let us recall that we aim at designing an automaton possibly involving state transition functions more general than T -functions. A shift is a special and trivial T -function. To this end, the following steps provide a way of adding edges $(\mathbf{v}^i, \mathbf{v}^j)$ while guaranteeing flatness.

Step 2: Add the edges $(\mathbf{v}^{r+i}, \mathbf{v}^{r+i+1})$ for $i = 1, \dots, n - r - 1$. Step 2 allows vertex \mathbf{v}^j , $j = r + 1, \dots, n$ to have a predecessor. Indeed, if not so, the dynamics of the corresponding vertex \mathbf{v}^j would reduce to $x_{k+1}^j = 0$ and would be clearly useless. The resulting path is a so-called main directed path and is depicted in Figure 3.

Step 3: Add the edges $(\mathbf{v}^r, \mathbf{v}^i)$, $i = 1, \dots, n$ that connect the vertex \mathbf{v}^r to any other vertices of the graph (except the vertex \mathbf{v}^0 related to the input).

Step 4: For every vertex \mathbf{v}^i , $i = 1, \dots, r - 1$, add the directed edge $(\mathbf{v}^i, \mathbf{v}^j)$ for $j = 1, \dots, i$.

The graph obtained after Step 1-4 is depicted in Figure 4.

Step 5: For every vertex \mathbf{v}^i , $i = r + 1, \dots, n$, add the directed edge $(\mathbf{v}^i, \mathbf{v}^j)$ for $j = 1, \dots, r$ and $j = i + 2, \dots, n$.

The resulting digraph after completion of Step 1-5 is depicted in Figure 5.

To sum up, the digraph $\mathcal{G}(\Sigma_\Lambda)$ is parametrized by the triplet (n, r, n_a) . The number of vertices of the digraph is equal to $n + 1$. Indeed, there are n vertices assigned to the state components and one assigned to the input. The delay r is the number of edges in the main directed path. The integer n_a defines the desired number of edges in the digraph $\mathcal{G}(\Sigma_\Lambda)$. It must satisfy $n_a \leq n_M$, where n_M is the maximal number of edges resulting from the construction Step 1-5. A simple counting leads to:

$$n_M = \frac{n(n+1)}{2} + r. \quad (30)$$

During the construction, at each step, we can decide whether we actually add the edges or not. That introduces flexibility in the perspective of providing distinct graphs and thus, distinct SSSC as detailed in Subsection II-C1.

Finally, the matrices I_A and I_B of the structural system Σ_Λ can be extracted from the adjacency matrix, denoted by \mathcal{I} , associated to the digraph $\mathcal{G}(\Sigma_\Lambda)$. Indeed, the adjacency matrix \mathcal{I} associated to the digraph $\mathcal{G}(\Sigma_\Lambda)$ is the $(n + 1) \times (n + 1)$ matrix

$$\mathcal{I} = \begin{pmatrix} 0 & \vdots \\ 0 & \vdots \\ \vdots & \vdots \\ 0 & \vdots \end{pmatrix} \quad (31)$$

where I_A^t and I_B^t stands respectively for the transpose of the structured matrices I_A and I_B . The entries \mathcal{I}_{ij} are defined as follows for $1 \leq i, j \leq n$

$$\mathcal{I}_{ij} = \begin{cases} 1 & \text{if there exists an edge from } \mathbf{v}^j \text{ to } \mathbf{v}^i \\ 0 & \text{otherwise.} \end{cases} \quad (32)$$

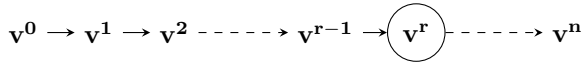
The adjacency matrix associated to $\mathcal{G}(\Sigma_\Lambda)$, obtained after completion of Step 1-5, is given by

$$\begin{matrix} & \mathbf{v}^0 & \mathbf{v}^1 & \mathbf{v}^2 & \mathbf{v}^3 & \dots & \mathbf{v}^r & \mathbf{v}^{r+1} & \dots & \mathbf{v}^{n-1} & \mathbf{v}^n \\ \mathbf{v}^0 & 0 & 1 & 0 & 0 & \dots & 0 & \dots & 0 & 0 & 0 \\ \mathbf{v}^1 & 0 & 1 & 1 & 0 & \dots & 0 & \dots & 0 & 0 & 0 \\ \mathbf{v}^2 & 0 & 1 & 1 & 1 & \dots & 0 & \dots & 0 & 0 & 0 \\ \mathbf{v}^3 & 0 & 1 & 1 & 1 & \dots & 0 & \dots & 0 & 0 & 0 \\ \vdots & \vdots & \vdots & \vdots & \vdots & \ddots & 0 & 0 & 0 & 0 & 0 \\ \mathbf{v}^r & 0 & 1 & 1 & 1 & \dots & 1 & 1 & 1 & 1 & 1 \\ \mathbf{v}^{r+1} & 0 & 1 & 1 & 1 & \dots & 1 & 0 & 1 & 1 & 1 \\ \vdots & \ddots & \ddots & \vdots \\ \mathbf{v}^{n-1} & 0 & 1 & 1 & 1 & \dots & 1 & 0 & 0 & 0 & 1 \\ \mathbf{v}^n & 0 & 1 & 1 & 1 & \dots & 1 & 0 & 0 & 0 & 0 \end{matrix}$$

The open source software Sagemath [34] has been used to elaborate the digraph $\mathcal{G}(\Sigma_\Lambda)$ corresponding to the triplet



Fig. 2. The Matrix A_S .



on the processors. It took 21 ms on the computer to obtain the digraph $\mathcal{G}(\Sigma_\Lambda)$.

Fig. 3. Digraph obtained after completion of Step 1-2. The vertex v^r corresponds to the flat output

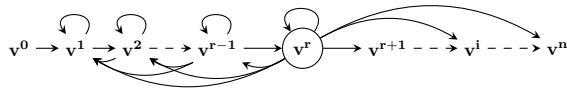


Fig. 4. Graph obtained after Step 1-4.

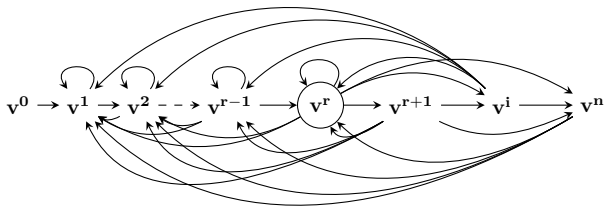


Fig. 5. Graph obtained after completion of Step 1-5.

($n = 40, r = 3, n_a = 120$). The construction has been performed on an Intel CORE i7 CPU 2.26 GHz running Linux Ubuntu 14.04. All experiments ran single-threaded